<center>**Supplementary information**</center>

Selective hydrogenation of nitroarenes to aminoarenes using MoO$_x$ modified Ru/SiO$_2$ catalyst under mild conditions

Masazumi Tamura, Naoto Yuasa, Yoshinao Nakagawa, Keiichi Tomishige

Department of Applied Chemistry, Graduate School of Engineering, Tohoku University, 6-6-07 Aoba, Aramaki, Aoba-ku, Sendai, 980-8579, Japan

1. General information

The GC (Shimadzu GC-2014)) and GC-MS (Shimadzu QP-5050) analyses were carried out with a CP-Sil5 capillary column (diameter 0.25 mmϕ, 50 m) using nitrogen for GC and helium for GC-MS as the carrier gases. All the chemicals for organic reactions were commercially available and were used without further purification.

2. Catalyst

M/SiO$_2$ (M = Ru, Rh, Pd, Pt, Ir) catalysts were prepared by impregnating SiO$_2$ (G-6, Fuji Silysia Chemical Ltd.) with an aqueous solution of Ru(NO)(NO$_3$)$_3$, RhCl$_3$·3H$_2$O, Pd(NO$_3$)$_2$, Pt(NH$_3$)$_4$(NO$_3$)$_2$ and H$_2$IrCl$_6$. M-M'O$_x$/SiO$_2$ (M'=Mo, Re and W) catalysts were prepared by impregnating M/SiO$_2$ after drying procedure with aqueous solutions of (NH$_4$)$_6$Mo$_7$O$_{24}$, NH$_4$ReO$_4$ and (NH$_4$)$_6$H$_2$W$_{12}$O$_{40}$. After the impregnation procedure and drying at 383 K for 12 h, the prepared catalysts were calcined under air at 773 K for 3 h. The loading amount of M in M-M'O$_x$/SiO$_2$ and M/SiO$_2$ was 4 wt%, and that of the additives was represented by the molar ratio of the additives to the noble metal. Carbon-supported noble metal catalysts (Ru/C, Pd/C, Rh/C and Pt/C) were commercially purchased from Wako Pure Chemical Industries, Ltd, and the loading amount of the noble metal was 5 wt%.

3. A typical procedure for hydrogenation of 3-nitrostyrene over Ru-MoO$_x$/SiO$_2$

Activity tests were performed in a 190-ml stainless steel autoclave with an inserted glass vessel. A reduced Ru-MoO$_x$/SiO$_2$ (typically 0.03 g), which was obtained after reduction at 473 K under H$_2$ flow for 1 h and passivation under 2% O$_2$/He flow for 10 min, and 3-nitrostyrene 0.45 g (3 mmol) were put into an autoclave together with a spinner. After sealing the reactor, the air content was quickly purged by flushing three times with 1 MPa hydrogen (99.99%; Nippon Peroxide Co., Ltd.). The autoclave was then heated to 303 K, and the H$_2$ pressure was increased to 0.3 MPa, and the temperature was monitored by using a thermocouple inserted in the autoclave. During the reaction, the stirring speed was fixed at 500 rpm (magnetic stirring). After the reaction, the gas phase was collected in a gas bag. The liquid phase in the autoclave was diluted with 10 g ethanol and transferred to a vial. The catalyst was separated by filtration. Details of the reaction conditions are described in each result. The products in the liquid phase and gas phase were analyzed by GC with CP-Sil5 (GL Sciences Inc.) and Porapak N (GL Science Inc.), respectively. Conversion of the substrate, and yield and selectivity of the products were determined by GC using 1,4-dioxane (~0.2 g) as an internal standard. TOF per surface Ru metal was denoted as TOF$_{sRu}$,

and was calculated by using the result of CO adsorption. TOF_{sRu} was calculated by the following equation: TOF_{sRu} (h^{-1}) = (Produced amount of 3-aminostyrene (mmol))/(surface Ru amount (mmol))/(Reaction time (h)). TOF, which was calculated per total Ru amount, was estimated by using the following equation: TOF (h^{-1}) = (Produced amount of 3-aminostyrene (mmol))/(Total Ru amount (mmol))/(Reaction time (h)). Reusability test of Ru-MoO$_x$/SiO$_2$(Mo/Ru=1/2) was carried out as follows: The catalyst can be easily retrieved from the reaction mixture by centrifugation. After washing with ethanol and reduction at 473 K under H$_2$, the recovered catalyst was reused for next reaction.

4. XRD, TEM(-EDX), TPR and CO adsorption experiment

X-ray diffraction (XRD) patterns were recorded by a diffractometer (MiniFlex600; Rigaku). Cu $K\alpha$ (λ = 0.154 nm, 45 keV, 40 mA) radiation was used as an X-ray source. Average metal particle size was estimated using the Scherrer's equation.

Field emission scanning transmission electron microscope (FE-STEM) images and energy-dispersive X-ray (EDX) analysis were obtained on a Hitachi spherical aberration corrected STEM/SEM HD-2700 instrument operated at 200 kV. After the reaction, the samples were dispersed in ethanol and placed on Cu grids under air atmosphere. Average particle size was calculated by $\Sigma n_i d_i^3 / \Sigma n_i d_i^2$ (d_i: particle size, n_i: number of particles with d_i). EDX analyses were performed using EMAX ENERGY EX-250 (Horiba Scientific).

Temperature-programmed reduction (TPR) was carried out in a fixed-bed reactor equipped with a frozen acetone trap and a thermal conductivity detector using 5% H$_2$ diluted with Ar (30 mL/min). The amount of catalyst was 0.1 g, and the temperature was increased from room temperature to 1073 K at a heating rate of 10 K/min.
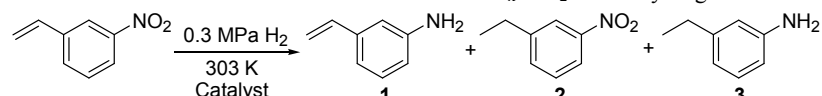
The amount of CO chemisorption was measured in a high-vacuum system using a volumetric method. The catalyst ($\approx$ 0.1 g) in the measurement cell was reduced with H$_2$ at 773 K for 1 h and evacuated at 773 K for 1 h. After cooling, the adsorption amount of CO was measured at room temperature. Gas pressure at adsorption equilibrium was about 1.1 kPa. The dead volume of the apparatus was about 60 cm^3.

5. XAS analysis

X-ray absorption spectroscopy (XAS) was conducted at the BL01B1 station in SPring-8 with the approval of the Japan Synchrotron Radiation Research Institute (JASRI; Proposal No. 2016A1352). The storage ring was operated at 8 GeV, and a Si (111) single crystal was used to obtain a monochromatic X-ray beam. Two ion chambers for I_0 and I were filled with 100% Ar and 80% Ar+20% Kr, respectively, for Ru K-edge measurement. Two ion chambers for I_0 and I were filled with 80% Ar+ 20% Kr and 50% Ar+ 50% Kr, respectively, for Mo K-edge measurement. We used the sample after the reduction and reaction. After the reduction or reaction, the catalyst powder was transferred to the measurement cell in a glove bag filled with nitrogen. The thickness of the cell filled with the powder was adjusted to give an edge jump of 0.2 ~ 1 for Ru K-edge and Mo K-edge measurement. The EXAFS data were collected in a transmission mode. For EXAFS analysis, the oscillation was first extracted from the EXAFS data using a spline smoothing method [1]. Fourier transformation of the k^3-weighted EXAFS oscillation from the k space to the r space was performed to obtain a radial distribution function. The inversely Fourier filtered data were analyzed using a usual curve fitting method [2,3]. For curve fitting analysis, the empirical phase shift and amplitude function for the Ru-Ru bond was extracted from the data for Ru powder. Analyses of EXAFS and XANES data were performed using a computer program (REX2000, ver. 2.6.0; Rigaku Corp.).

6. Supplementary Tables

Table S1 Effect of molar ratio of M'/Ru in Ru-M'O$_x$/SiO$_2$ on the hydrogenation of 3-nitrostyrene

Catalyst	Molar ratio (M'/Ru)	Conversion (%)	Selectivity (%)			
			1	2	3	Others
Ru/SiO$_2$	0	5.2	80.0	6.8	0.5	12.7
Ru-MoO$_x$/SiO$_2$	1/32	13.3	99.2	0.5	0.3	<0.1
	1/16	27.2	98.0	0.2	0.2	1.6
	1/8	27.3	98.6	0.1	0.2	1.2
	1/2	25.8	99.2	0.1	0.1	0.2
	1	14.3	99.2	0.3	0.5	<0.1
Ru-WO$_x$/SiO$_2$	1/32	22.7	96.3	0.8	0.4	2.5
	1/16	32.2	97.4	0.4	0.5	1.8
	1/8	34.1	98.1	0.3	0.5	1.1
	1/2	28.7	98.4	0.2	0.6	0.8
	1	11.9	99.4	<0.1	<0.1	0.6
Ru-ReO$_x$/SiO$_2$	1/32	11.2	86.6	2.4	0.4	10.6
	1/16	19.0	96.0	1.1	0.3	2.5
	1/8	24.3	99.1	0.2	0.2	0.5
	1/2	13.4	99.5	<0.1	<0.1	0.5
	1	10.5	>99.9	<0.1	<0.1	<0.1

Reaction conditions: 3-nitrostyrene 3 mmol, catalyst (Ru=4 wt%) 30 mg, 303 K, H$_2$ 0.3 MPa, 6 h. Others: mainly 3-nitrosostyrene.

Table S2 Reusability test of Ru-MoO$_x$/SiO$_2$(Mo/Ru=1/2) catalyst in hydrogenation of 3-nitrostyrene

Usage time	Conversion (%)	Selectivity (%)			
		1	2	3	Others
First	25.8	99.2	0.1	0.1	0.2
Second	21.8	98.4	<0.1	0.3	1.2

Reaction conditions: 3-nitrostyrene 3 mmol, Ru-MoO$_x$/SiO$_2$(Mo/Ru=1/2) 30 mg, 303 K, H$_2$ 0.3 MPa, 6 h. Others: mainly 3-nitrosostyrene.

Table S3 Effect of solvents in hydrogenation of 3-nitrostyrene over Ru-MoO$_x$/SiO$_2$(Mo/Ru=1/2)

Solvent	Conversion (%)	Selectivity (%)			
		1	2	3	Others
None (neat)	25.8	99.2	0.1	0.1	0.2
Water	26.9	97.9	<0.1	1.2	1.0
Toluene	23.6	99.3	0.5	0.2	<0.1
1,2-Dimethoxyethane	4.6	91.4	2.2	<0.1	6.4
THF	2.1	92.2	<0.1	<0.1	7.8
Ethanol	2.0	93.2	<0.1	<0.1	6.8
1-Propanol	2.0	93.2	<0.1	<0.1	6.8

Reaction conditions: 3-nitrostyrene 3 mmol, Ru-MoO$_x$/SiO$_2$(Mo/Ru=1/2) 30 mg, solvent 3 g or 0 g, 303 K, H$_2$ 0.3 MPa, 6 h. Others: 3-nitrosostyrene and 3-ethyl-N-hydroxyaniline.

Table S4 Characterization results of the catalysts by XRD, TEM and CO adsorption

Catalyst	Mo/Ru	d (XRD)[a] (nm) after reduction	d (XRD)[a] (nm) after reaction	d (TEM)[b] (nm) *after reaction*	CO adsorption (CO/Ru)	Valence of Mo (TPR)
Ru/SiO$_2$	0	5.1	5.5	5.1	0.14	-
Ru-MoO$_x$/SiO$_2$	1/32	5.1	-	-	0.13	5
	1/16	5.4	-	-	0.11	4
	1/8	5.4	-	-	0.07	5
	1/2	5.1	5.2	5.0	0.04	5
	1	5.4	-	-	-	-

[a]Particle size of Ru was calculated from XRD analyses. [b]Particle size of Ru was calculated from TEM image.
Valence of Mo after TPR was calculated by 6-(H$_2$ consumption [mol]$\times$ 2 - Ru amount [mol]$\times$ 4)/(Mo amount [mol]).

Table S5 Curve fitting results for the Ru-K edge EXAFS analysis of Ru–MoO$_x$/SiO$_2$(Mo/Ru=1/2).

Catalyst	Shells	CN[a]	R (10^{-1} nm)[b]	σ (10^{-1} nm)[c]	ΔE_o (eV)[d]	R_f (%)[e]
Ru–MoO$_x$/SiO$_2$(Mo/Ru=0.5) after reaction	Ru–Ru (or –Mo)	11.6	2.67	0.066	-0.5	0.9
Ru–MoO$_x$/SiO$_2$(Mo/Ru=0.5) after reduction	Ru–Ru (or –Mo)	11.7	2.67	0.067	-0.5	0.9
Ru powder	Ru–Ru	12	2.68	0.060	0	-

[a]Coordination number.

[b]Bond distance.

[c]Debye-Waller factor.

[d]Difference in origin of photoelectron energy between the reference and the sample.

[e]Residual factor.

Fourier filtering range: 0.153-0.303 nm.

Table S6 Effect of substrate concentration in hydrogenation of 3-nitrostyrene over Ru/SiO$_2$

Substrate concentration (M)	t (h)	Conversion (%)	Selectivity (%)				TOF (h^{-1})
			1	**2**	**3**	Others	
0.5	6	2.0	59.9	19.3	1.4	19.4	0.5
1.0	8	4.9	72.8	8.8	1.2	17.2	1.0
2.0	6	5.0	68.4	7.5	0.9	23.2	1.4

Reaction conditions: 3-nitrostyrene 3 mmol, Ru/SiO$_2$ 30 mg, 303 K, H$_2$ 0.3 MPa, toluene 1.5-6 g. Others: mainly 3-nitrosostyrene.

Table S7 Effect of substrate concentration in hydrogenation of 3-nitrostyrene over Ru-MoO$_x$/SiO$_2$

Substrate concentration (M)	t (h)	Conversion (%)	Selectivity (%)				TOF (h^{-1})
			1	(h^{-1})	**3**	Others	
0.5	6	21.6	97.5	0.2	0.8	1.6	9.5
1.0	6	23.6	98.0	0.1	0.8	1.1	9.4
2.1	6	23.3	98.0	<0.1	1.1	0.9	8.0

Reaction conditions: 3-nitrostyrene 3 mmol, Ru-MoO$_x$/SiO$_2$ 30 mg, 303 K, H$_2$ 0.3 MPa, toluene 1.5-6 g. Others: mainly 3-nitrosostyrene.

Table S8 Effect of H$_2$ pressure concentration in hydrogenation of 3-nitrostyrene over Ru/SiO$_2$

H$_2$ pressure (MPa)	t (h)	Conversion (%)	Selectivity (%)				TOF (h^{-1})
			1	**2**	**3**	Others	
0.3	2	2.8	73.4	9.5	<0.1	17.1	2.5
1.0	2	7.7	57.6	8.7	0.9	28.3	5.3
3.0	2	15.7	54.6	7.0	1.3	27.0	10

Reaction conditions: 3-nitrostyrene 3 mmol, Ru/SiO$_2$ 30 mg, 303 K, H$_2$ 0.3 MPa. Others: mainly 3-nitrosostyrene.

Table S9 Effect of H$_2$ pressure concentration in hydrogenation of 3-nitrostyrene over Ru-MoO$_x$/SiO$_2$

H$_2$ pressure (MPa)	t (h)	Conversion (%)	Selectivity (%)				TOF (h^{-1})
			1	**2**	**3**	Others	
0.3	2	8.2	99.7	<0.1	0.3	<0.1	9.7
1.0	2	30.0	97.5	0.2	0.5	1.8	34
3.0	1	30.3	96.2	0.1	0.8	2.9	70

Reaction conditions: 3-nitrostyrene 3 mmol, Ru-MoO$_x$/SiO$_2$ 30 mg, 303 K, H$_2$ 0.3 MPa. Others: mainly 3-nitrosostyrene.
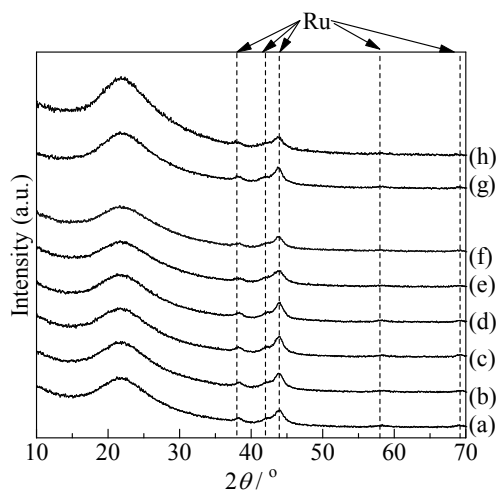
7. Supplementary Figures

Figure S1 XRD profiles of Ru-MoO$_x$/SiO$_2$(Mo/Ru=0-1) after reduction and reaction.
The samples after reduction: (a) Ru/SiO$_2$, (b) Ru-MoO$_x$/SiO$_2$(Mo/Ru=1/32), (c) Ru-MoO$_x$/SiO$_2$(Mo/Ru=1/16), (d) Ru-MoO$_x$/SiO$_2$(Mo/Ru=1/8), (e) Ru-MoO$_x$/SiO$_2$(Mo/Ru=1/2), (f) Ru-MoO$_x$/SiO$_2$(Mo/Ru=1). The samples after reaction: (g) Ru/SiO$_2$, (h) Ru-MoO$_x$/SiO$_2$(Mo/Ru=1/2).
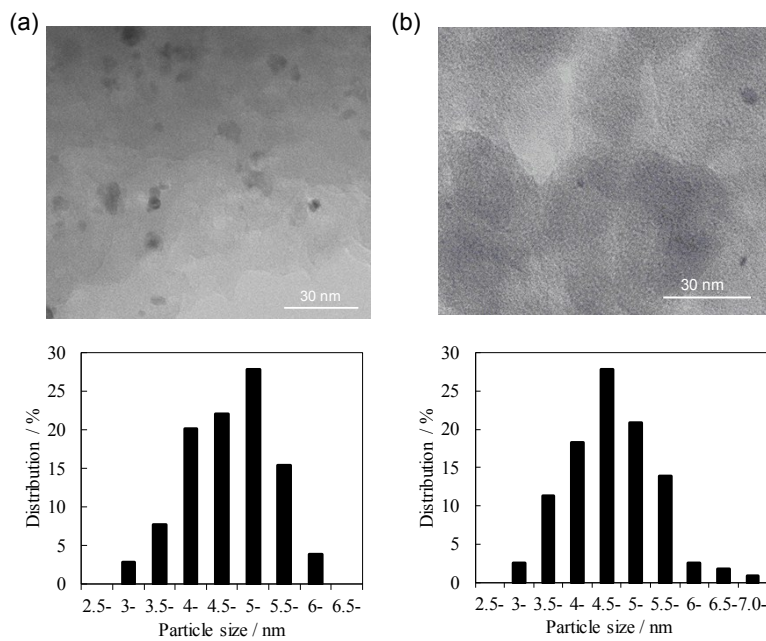
Figure S2 TEM images and distribution of Ru particles of Ru/SiO$_2$ (a) and Ru-MoO$_x$/SiO$_2$(Mo/Ru=1/2) (b) after reaction.

(a)

50 nm

(b)

(c)

(d)
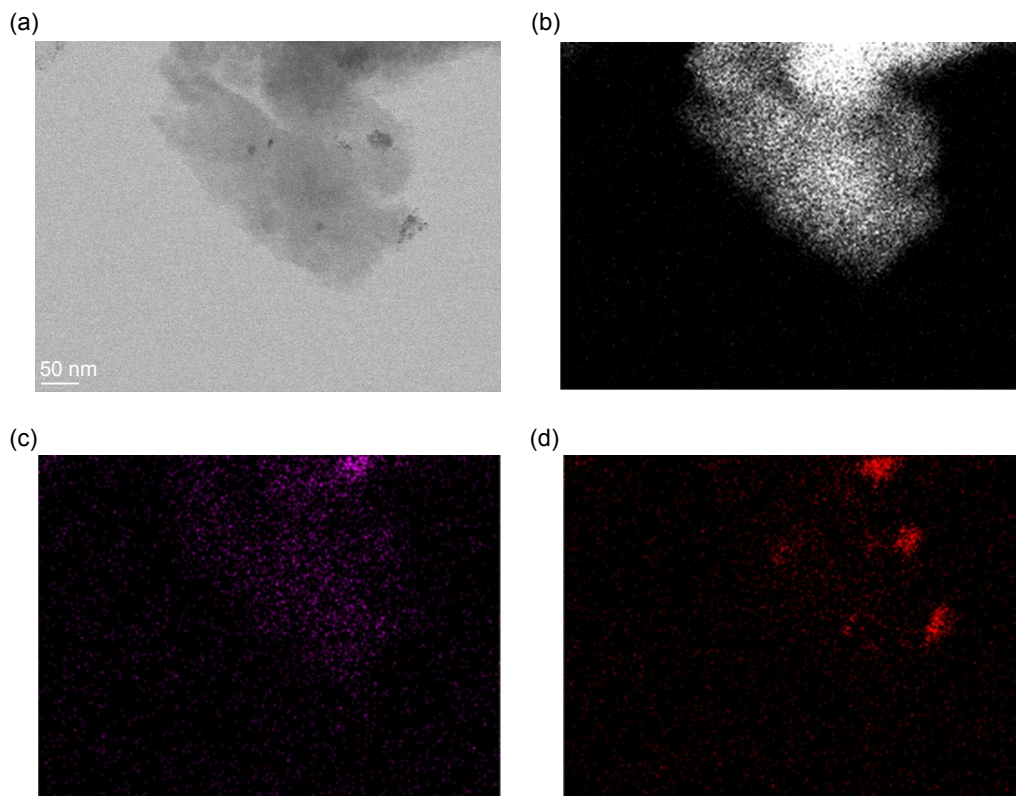
Figure S3 TEM-EDX images of Ru-MoO$_x$/SiO$_2$(Mo/Ru=1/2) after reaction. (a) TEM image, (b) Si elemental mapping, (c) Mo elemental mapping, (d) Ru elemental mapping.
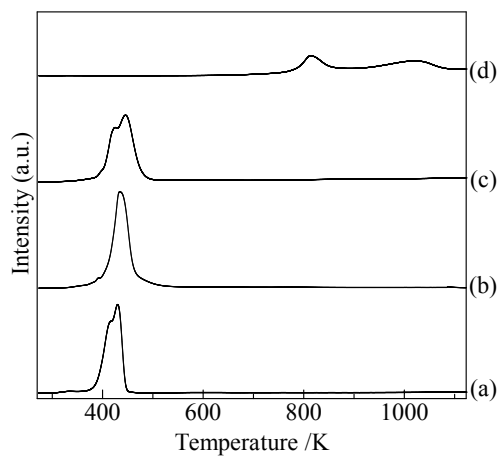
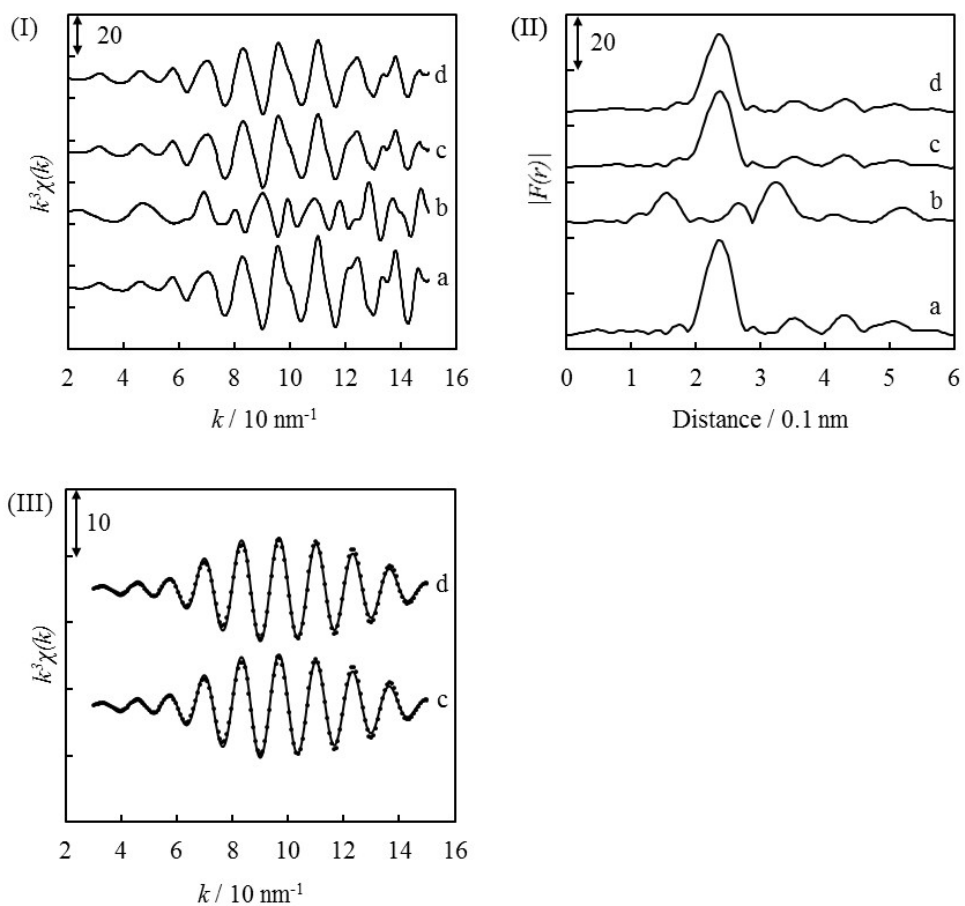Figure S4 TPR profiles of Ru/SiO$_2$ (a), Ru-MoO$_x$/SiO$_2$(Mo/Ru=1/8) (b), Ru-MoO$_x$/SiO$_2$(Mo/Ru=1/2) (c) and MoO$_x$/SiO$_2$ (d)

Figure S5 Ru-*K* edge EXAFS analysis of Ru–MoO$_x$/SiO$_2$(Mo/Ru=1/2) and reference samples

(I) k^3-Weighted EXAFS oscillations. (II) Fourier transform of k^3-weighted Re L_3-edge EXAFS, FT range: 30–150 nm^{-1}. (III) Fourier filtered EXAFS data (solid line) and calculated data (dotted line).

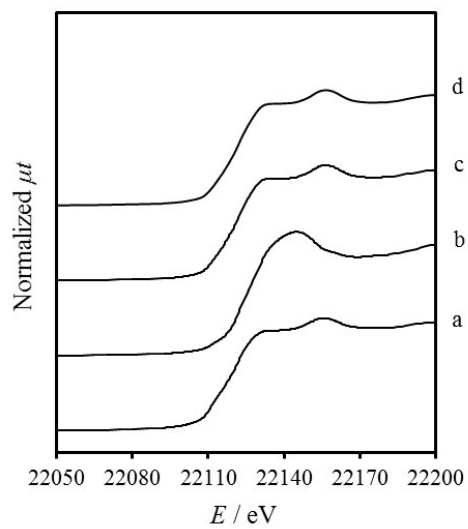(a) Ru powder, (b) RuO$_2$, (c) Ru–MoO$_x$/SiO$_2$(Mo/Ru=1/2) after reduction, (d) Ru–MoO$_x$/SiO$_2$(Mo/Ru=1/2) after reaction.

Figure S6 Ru-*K* edge XANES spectra of Ru–MoO$_x$/SiO$_2$(Mo/Ru=1/2) and reference samples

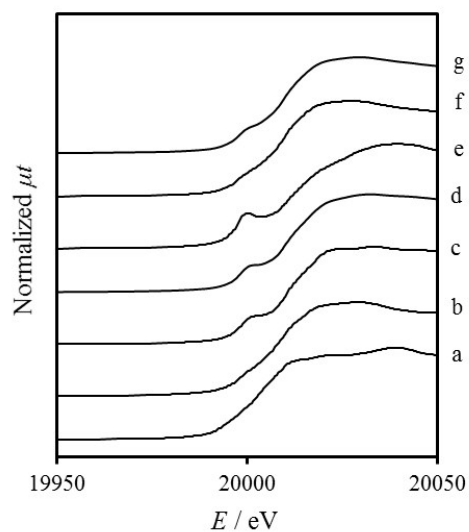(a) Ru powder, (b) RuO$_2$, (c) Ru–MoO$_x$/SiO$_2$(Mo/Ru=1/2) after reduction, (d) Ru–MoO$_x$/SiO$_2$(Mo/Ru=1/2) after reaction.

Figure S7 Mo-*K* edge XANES spectra of Ru–MoO$_x$/SiO$_2$(Mo/Ru=1/2) and reference samples

(a) Mo foil, (b) MoO$_2$, (c) MoO$_3$, (d) Na$_2$MoO$_4$, (e) (NH$_4$)$_6$Mo$_7$O$_{24}$, (f) Ru–MoO$_x$/SiO$_2$(Mo/Ru=1/2) after reduction, (g) Ru–MoO$_x$/SiO$_2$(Mo/Ru=1/2) after reaction.
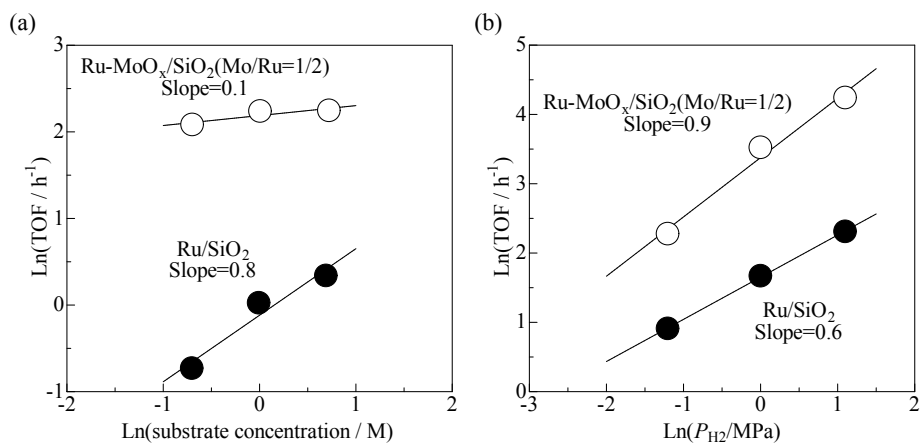
Figure S8 Effect of 3-nitrostyrene concentration (a) and H$_2$ pressure (b) over Ru/SiO$_2$ and Ru-MoO$_x$/SiO$_2$(Mo/Ru=1/2)
The detailed data are shown in Tables S6-9.

8. References

[1] J. W. Cook Jr and D. E. Sayers, *J. Appl. Phys.*,1981, **52**, 5024.

[2] K. Okumura, J. Amano, N. Yasunobu and M. Niwa, *J. Phys. Chem. B*, 2000, **104**, 1050.

[3] K. Okumura, S. Matsumoto, N. Nishiaki, M. Niwa, *Appl. Catal. B*, 2003, **40**, 151.